Journal of Alloys and Compounds, *195* (1993) 499–502
JALCOM 7514

Characterization of superconductors using magnetooptic techniques

M.V. Indenbom,[a] * A.Forkl,[a] H.-U.Habermeier[b] and H.Kronmüller[a]

[a]Max-Planck-Institut für Metallforschung, Institut für Physik, [b]Max-Planck-Institut für Festkörperforschung
Heisenbergstrasse 1, 7000 Stuttgart 80, F.R.G.

Abstract

Direct observations and measurements of spatial magnetic flux distributions on the surfaces of YBaCuO superconducting thin films and thin single crystals realized under application of external magnetic field and transport current are accomplished using magneto-optical indicators. These investigations are compared with theoretical calculations yielding critical current densities. Special attention is paid to the influence of defects on the magnetic properties. Furthermore, specific features of flux penetration into flat superconductors are revealed.

1. Introduction

More information to reconstruct a true model of magnetization of superconductors can be obtained from direct observations of the magnetic flux structure on their surface using the magnetooptic techniques [1]. High-T_c superconductors are investigated by both the traditional $EuS{:}EuF_2$ and EuSe indicator films deposited directly onto the sample surface [2] and newly used for this purpose much more sensitive garnet ferrimagnetic films [3,4]. To determine the correct superconducting parameters values from the field distribution the strong influence of demagnetization factors must be taken into account [5,6]. The purpose of this paper is to demonstrate the new possibilities of the magnetooptical method to characterize superconductors, especially to reveal the influence of defects and inhomogeneities, and to measure the intrinsic parameters of the superconductor independently from macrodefects. The main problem in interpretation of magnetooptic observations is the calculation of the current distribution from the normal component of the flux. Both a fitting procedure [6] and recently obtained integral equations [7] are, so called, mathematically incorrect problems and the results contradict with traditional magnetic measurements [6]. For correct interpretation of the experiments new solutions of the critical state model are made for a thin film stripe.

2. Experimental techniques

Details of the apparatus and the experimental procedure can be found in [1,2,4,8,9]. As magnetooptic active medium we use both the vapor-deposited EuSe films and the ferrimagnetic garnet indicator with in-plane anisotropy. The highest optical resolution can only be obtained with EuSe which is magnetooptically active only near liquid helium temperature. To apply it also for higher temperatures a special new procedure was developed. Flux structures realized at a temperature where the EuSe indicator is insensitive are observed after cooling down to liquid helium temperature. Applicability of the procedure was checked by the garnet indicator.

3. Results and discussion

3.1. *Magnetic flux of transport current*

Direct study of the self magnetization of a type II superconductor carrying transport current can be very useful in understanding features of the critical current formation, being of great importance for practical application. It became possible only recently using the in-plane garnet indicator [10]. We perform such observations to investigate the critical regime formation in $YBa_2Cu_3O_7$ thin film bridges with linear defects, which are often clearly observed magnetooptically in high-T_c films due to easier field penetration along them [8,11]. Magnetic field induced by the applied transport current penetrates into the linear defect, being a narrow weak superconducting region of the film near a tiny scratch onto the substrate surface that existed before the film preparation. After reducing the current the penetrated flux is captured in the film. Fig.1 shows that the magnetic irreversibility during the current changes takes place only in the defect, although there is no barrier for the flux entrance in thin films and penetrated flux could be captured at the edges also. Even after reaching the critical current value of 0.5 – 1.5 A in the investigated thin film bridges no captured flux at the bridge edges were detected. The observed reversibility in "ideal" parts of the sam-

---

*Under the financial support of the Alexander von Humboldt Foundation. Permanent address: Institute of Solid State Physics, Russian Academy of Science, 142432 Chernogolovka, Moscow distr., Russia.

0925-8388/93/$06.00

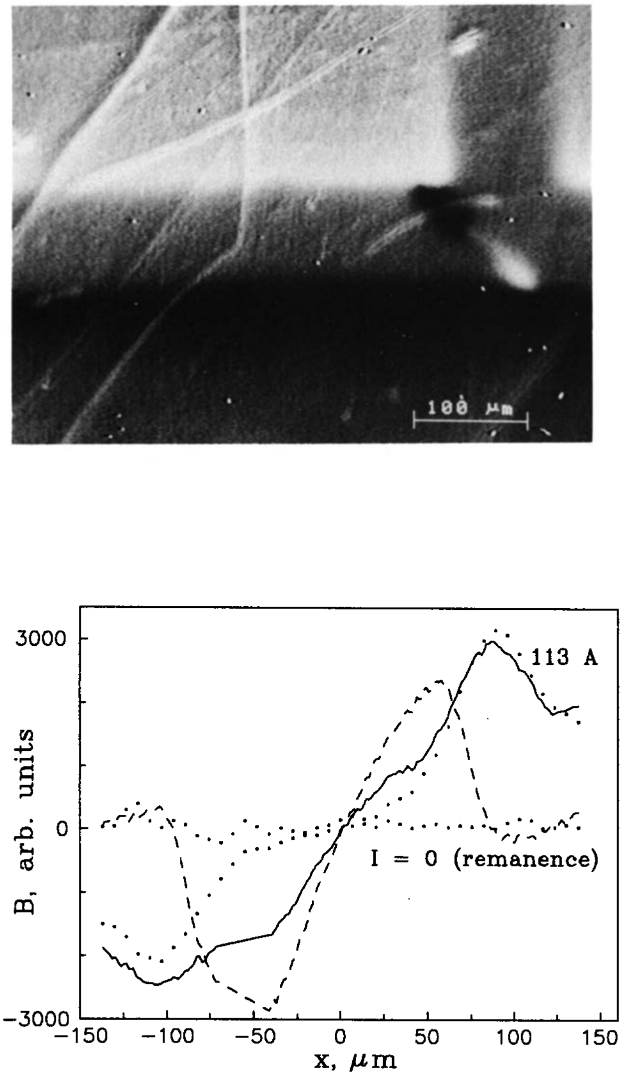

Figure 1. *Up*: The flux structure from current of 50 mA in an YBaCuO thin film bridge after the critical current −500 mA was applied in the opposite direction (the film thickness is 210 nm, width - 96 μm, T = 5 K). The fields of opposite polarity above and below the bridge are visible as light and dark regions due to Faraday effect in the indicator. Reverse contrast black-white petals represent remanent flux penetrated and captured along a linear defect near a potential contact, revealed as gray vertical stripe screening the field of the current. *Down*: flux profiles measured along the defect in presence of a current 113 mA applied to the sample just zero field cooled (solid line) and after switching off the maximal current 500 mA (dashed line). Dotted lines are the corresponding profiles far from the defect.

ple [12] can be explained taking into account the analytical solution of the critical state model in this case [13] giving the initial flux penetration depth proportional only to square of the current. Thus, macrodefects define not only the evident reduction of the critical current value obtained by transport measurements but also AC electrical losses in thin film stripes at current amplitudes *lower than the critical value.*

3.2. Flux penetration into thin films

One can measure the intrinsic value of the critical current density independently on macrodefects only visualizing the flux penetration and capture under external magnetic field, B_a (Fig.2a). The simplest way is then to compare the flux profile measured in the fully critical state with the field distribution calculated analytically from the critical current flowing with constant density, j_c, troughout the sample [14,15]. In the case of thin film stripe the spatial distribution of the normal field has very simple analytical form [5]:

$$B_z(x) = \pm(\mu_0/2\pi)tj_c{\cdot}ln \mid 1-\left(\frac{w/2}{x-w/2}\right)^2 \mid +B_a,$$

where $0 < x < w, w$ – the stripe width; '+' or '−' sign takes place at decrease or increase of the B_a, correspondingly. Fitting the measured flux profile in remanent state with this theoretical one ('+' sign, $B_a = 0$) we obtained the value of critical current density of $1.4{\cdot}10^7 A/cm^2$ (Fig.2b). But before this procedure the correct calibration of measured light intensity from the field has to be done in each experiment. This makes the measurements too time consuming and complicated (changes of the intensity amplification made by the camera and the following path of the video signal as well as light instability should be taken into account). We have numerically calculated flux penetration into a superconducting thin film stripe of width, w, and thickness, t, under applied field, supposing critical current density independence from field [16]. The obtained flux profiles are essentially nonlinear even on early stage of the flux penetration. It should be mentioned here that due to the latter fact measurements of j_c simply from $\partial B_z/\partial x$ are impossible. From the theoretical profiles flux penetration depth, x_p, was determined. Comparison of the universalized curve $x_p(H_a/j_ct)/w$ with measured x_p gives the critical current density of $1.3{\cdot}10^7$ A/cm^2 (Fig.2c) that is in very good agreement with the profile fitting (Fig.2b). Moreover, on Fig.2c one can see very slow initial flux penetration proportional to B_a^2 that is of the same nature as the I^2 flux penetration under transport current calculated a long time ago [13], the former being not well known. This fact can explain the characteristic features of magnetization curves of thin high-T$_c$ single crystals without any special supposition of a surface

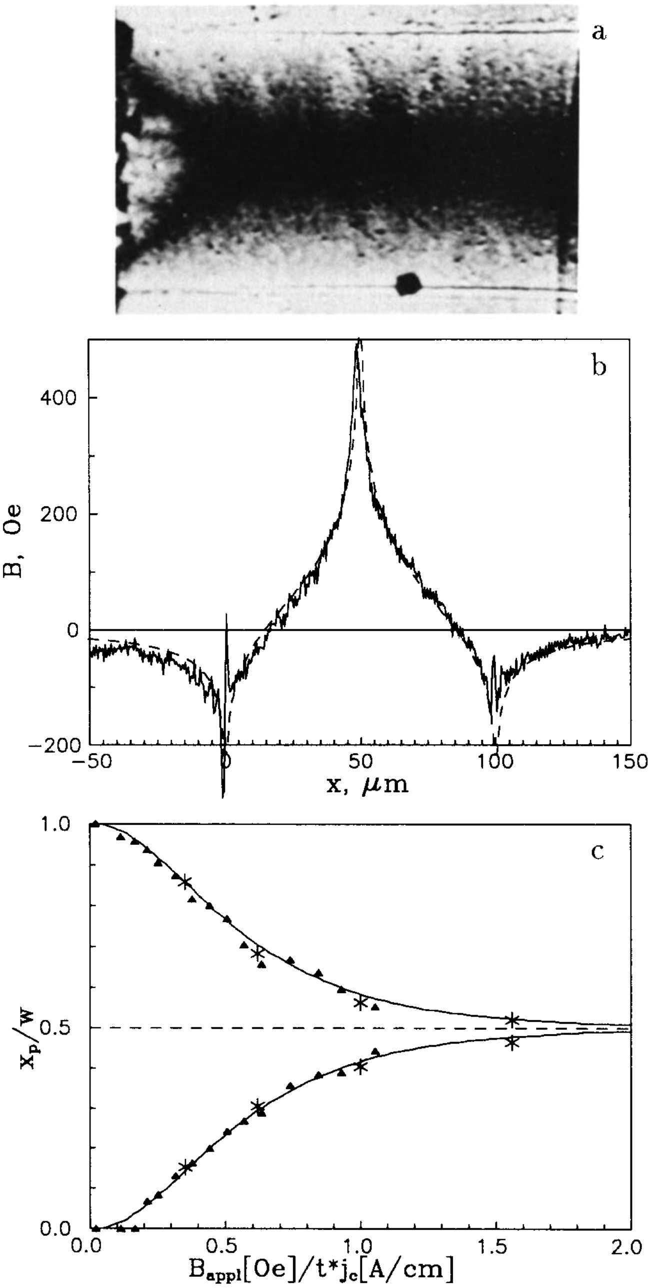

Figure 2. a) Flux structure in an YBaCuO thin film stripe (the film thickness $t =$ 200 nm, width $w = 100\mu$m) observed under $B_a = 155$ Oe at T = 5 K using the EuSe indicator. Meissner phase in the center of the superconductor is dark, Shubnikov phase and the flux around it are bright. The stripe edges are seen as tiny black lines. b) Flux profile measured across the bridge in the remanent state from a high field. Dashed line is the theoretical fitting. c) Calculated dependence $x_p(B_a)$ and corresponding experimental points obtained on the bridge ($*$) and on another one (▲ – $w = 180\mu$m, t = 540 nm, $j_c = 3.7{\cdot}10^7$A/cm^2).

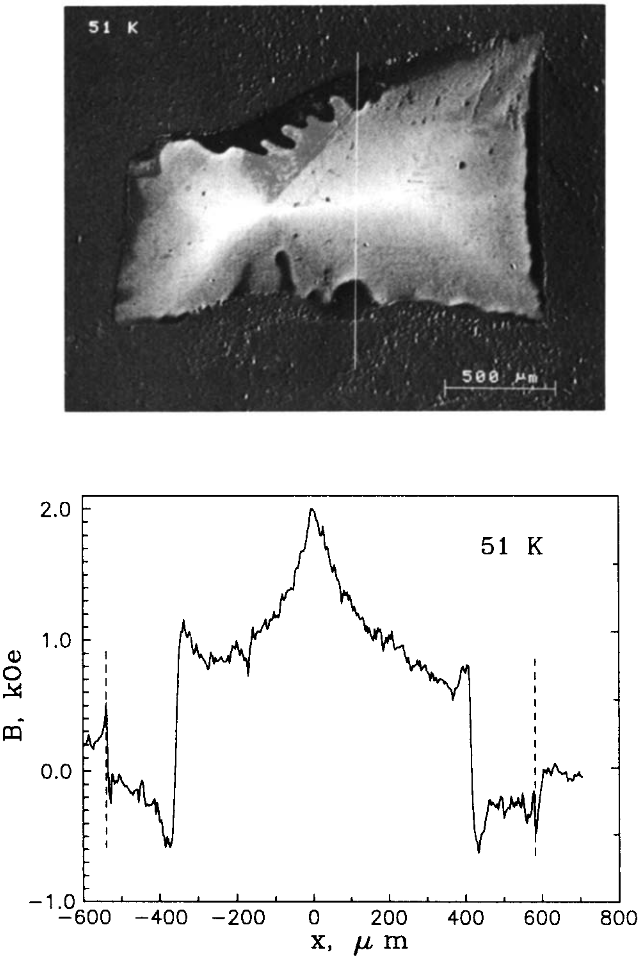

Figure 3. Flux structure in the remanent state of an YBaCuO crystal at 51 K and the corresponding profile measured along the indicated line. The sharp wall (< 1μm as was proved at higher magnification) divides the negative flux domain (dark) and the captured flux (bright). Bright lines of the characteristic form in the sample center and the corresponding peak of the profile reveal the boundary of critical current direction switching [10].

barrier existence [17,18] and can be a key to solution of the problem of the anomalous penetration field upturn at low temperatures (see [17,18] and references there).

3.3. *Flux structure in single crystals*

Of course the flux structure in single crystals is somewhat more complicated, the first critical field, H_{c1}, and the volume vortex interactions being involved. Earlier the most interesting temperature region for high-T_c superconductors was possible to investigate only using indicator garnet films [3,4, 8,10]. Now we have for the first time visualized magnetic flux structure with higher spatial resolution at high temperatures using the method of freezing. In contrast to flux profiles in thin films the one obtained in an $YBa_2Cu_3O_7$ single crystal have a very sharp magnetic wall of irregular form between fluxes of opposite polarities (Fig.3). This wall is more pronounced near 50 K, where the pinning density is already low but H_{c1} is still high, and can move honey-like through the crystal under applied field. An influence of twins is also perceptible, twin free regions obtain lower pinning and the wall curvature amplitude is in these places higher. We believe that this sharp magnetic wall exists due to softening of the vortex lattice at low fields [19] and should define characteristic features of superconductor magnetization curves in this region.

4. Acknowledgements

The authors would like to thank T. Dragon, B. Leibold and R. Knorpp for technical assistance and A.V. Antonov and M.Ju. Gusev of the scientific production firm "Gamma" (Moscow) for supplying with the in-plane garnet indicatior.

We are grateful to Mary Carpenter and Marianne van der Ploeg of the Elsevier Science Publishers B.V. Camera-Ready Publications Department for sending us the LaTeX style file *"espcrc2.sty"* by P. de Groot and X.-Y. Wang. This paper was prepared only with slight modifications of the file.

REFERENCES

1 R.P. Huebener, Magnetic Flux Structures in Superconductors, Springer-Verlag, Berlin, 1979; H.-U. Habermeier and H. Kronmüller, Appl. Phys. 12 (1977) 297.

2 N. Moser, M.R. Koblischka, H. Kronmüller, B. Gegenheimer and H. Theuss, Physica C, 159 (1989) 117; Th. Schuster, M.R. Koblischka, B. Ludescher and H. Kronmüller, J. Appl. Phys., 72 (1992) 1478. A. Forkl, T. Dragon, H. Kronmüller, H.-U. Habermeier and G. Mertens, Appl. Phys. Lett., 57 (1990) 1067;

3 A.A. Polyanskii, V.K. Vlasko-Vlasov, M.V. Indenbom and V.I. Nikitenko, Sov. Tech. Phys. Lett., 15 (1989) 872.

4 A.A. Polyanskii, L.A. Dorosinskii, M.V. Indenbom, V.I. Nikitenko, Ju.A. Ossip'yan, V.K. Vlasko-Vlasov and H.-U. Habermeier, in: High-T_c Superconductor Thin Films (Proceedings of Symposium A1 on High Temperature Superconductor Thin Films of the International Conference on Advanced Materials — ICAM 91, Strasbourg, France, 27–31 May, 1991), North-Holland, Amsterdam, 1992.- p.195; L.A. Dorosinskii, M.V. Indenbom, V.I. Nikitenko, Yu.A. Ossip'yan, A.A. Polyanskii and V.K. Vlasko-Vlasov, Physica C, 203 (1992) 149.

5 L.T. Baczewsky, K. Piotrovski, R. Szymczak, H. Szymczak and A.P. Malozemoff, Physica C, 175 (1991) 363.

6 H. Theuss, A. Forkl and H. Kronmüller, Physica C, 190 (1992) 614.

7 E.-H. Brandt, Phys. Rev. B, 46 (1992) 8628.

8 M.V. Indenbom, N.N. Kolesnikov, M.P. Kulakov, I.G. Naumenko, V.I. Nikitenko, A.A. Polyanskii, N.F. Vershinin, and V.K. Vlasko-Vlasov, Physica C, 166 (1990) 486.

9 Th. Schuster, M.R. Koblischka, B. Ludescher, N. Moser and H. Kronmüller, Cryogenics, 31 (1991) 811.

10 V.K. Vlasko-Vlasov, M.V. Indenbom, V.I. Nikitenko, A.A. Polyanskii, R.L. Prozorov, I.V. Grechov, L.A. Delimova, I.A. Liniichuk, A.V. Antonov, M.Ju. Gusev, Superconductivity (physics, chemistry, technique), 5 (1992) 1637.

11 A. Forkl, T. Dragon and H. Kronmüller, J. Appl. Phys., 67 (1990) 3047.

12 M.V. Indenbom, A. Forkl and H. Kronmüller, Submitted to J. of Superconductivity.

13 W.T. Norris, J. Phys. D, 3 (1970) 489.

14 A. Forkl, H.-U. Habermeier, B. Leibold and H. Kronmüller, Physica C, 185-189 (1991) 2335.

15 P. Brüll, D. Kirchgüssner and P. Leiderer, Physica C, 195 (1991) 157

16 M.V. Indenbom, A. Forkl and H. Kronmüller, to be published.

17 L. Burlachkov, Y. Yeshurun, M. Konczykowski and F. Holtzberg, Phys. Rev. B, 45 (1992) 8193.

18 V.N. Kopylov, A,E. Koshelev, I.F. Schegolev and T.G. Togonidze, Physica C, 170 (1990) 291.

19 H. Ullmaier, Irreversible Properties of Type-II Superconductors, Springer, Berlin, 1975.